MOLECULAR GAS AND THE NUCLEAR STAR CLUSTER IN IC 342: SUFFICIENT INFLOW FOR RECURRING STAR FORMATION EVENTS?

EVA SCHINNERER,[1,2] TORSTEN BÖKER,[3,4] AND DAVID S. MEIER[5]

ABSTRACT

We present high spatial resolution (1″.2) millimeter-interferometric observations of the ^{12}CO (2–1) line emission in the central 300 pc of the late-type spiral galaxy IC 342. The data, obtained with the Owens Valley Radio Observatory, allow first-time detection of a molecular gas disk that coincides with the luminous young stellar cluster in the nucleus of IC 342. The nuclear CO disk has a diameter of ~30 pc and a molecular gas mass of $M_{H_2} \sim 2 \times 10^5\ M_\odot$. It connects via two faint CO bridges to the well-known 100 pc diameter circumnuclear gas ring. Analysis of the gas kinematics shows that the line of nodes in the inner 15 pc is offset by about 45° from the major kinematic axis, indicating noncircular motion of the gas within a few parsecs of the dynamical center of IC 342. Both the morphology and the kinematics of the CO gas indicate ongoing inflow of molecular gas into the central few parsecs of IC 342. We infer a gas inflow rate between 0.003 and 0.14 $M_\odot$ yr^{-1}, based on the observed surface density of the nuclear gas disk and estimates of the radial velocities of the surrounding gas. Inflow rates of this order can support repetitive star formation events in the nucleus of IC 342 on timescales much smaller than a Hubble time.

Subject headings: galaxies: individual (IC 342) — galaxies: ISM — galaxies: kinematics and dynamics — galaxies: nuclei

1. INTRODUCTION

Recent observations with the *Hubble Space Telescope* (*HST*) at both optical and near-infrared wavelengths (e.g., Carollo, Stiavelli, & Mack 1998; Böker et al. 2002) have revealed that the very centers of late-type spiral galaxies are often occupied by a photometrically distinct, luminous, and compact (with a few parsec diameter) stellar cluster. Most of the nuclear star clusters studied in detail appear to have experienced recent star formation. For example, M33 (Gordon et al. 1999), NGC 4449 (Böker et al. 2001), as well as NGC 247 and NGC 2403 (Davidge & Courteau 2002), all have nuclear clusters with a spectral energy distribution (SED) that is dominated by a young (≲100 Myr) stellar population. Clearly, these galaxies must recently have experienced significant inflow of molecular gas into their central few parsecs in order to trigger the formation of these young clusters. There is mounting evidence that large-scale bars can efficiently move large quantities of molecular gas down to the inner kiloparsec (Sakamoto et al. 1999). However, the exact mechanism that can transport gas from a few hundred parsecs down to a few parsecs is still under debate.

IC 342 is a prime example of a late-type spiral galaxy with a young luminous nuclear cluster that formed in a short-lived burst about 60 Myr ago (Böker, Förster-Schreiber, & Genzel 1997; Böker, van der Marel, & Vacca 1999). For this Letter, we adopt the distance of 1.8 Mpc derived by McCall (1989), which makes IC 342 the closest late-type galaxy with strong nuclear star formation.[6] It thus offers a unique opportunity to study the related gasdynamics on scales of a few parsecs (1″ ~ 8.7 pc). The central region of IC 342 has been mapped in the past in several molecular transitions on scales of a few arcseconds (e.g., Lo et al. 1984; Ishizuki et al. 1990; Turner & Hurt 1992; Turner, Hurt, & Hudson 1993; Meier, Turner, & Hurt 2000; Meier & Turner 2001). These maps show that the molecular gas is located in two spiral arms that show strong streaming motions. The spiral arms join to form a ring of about 10″ diameter that is the site of massive star formation (Böker et al. 1997). In this Letter, we present a high-resolution high-sensitivity ^{12}CO (2–1) map that for the first time resolves the molecular gas kinematics *inside* the starburst ring.

2. OBSERVATIONS

The center of IC 342 was observed in the ^{12}CO (2–1) line in 2002 January with the six-element Owens Valley Radio Observatory (OVRO) millimeter interferometer. Obtained in the L and H configurations with baselines between 15 and 115 m, the data have a spatial resolution of ~1″.2 (10 pc) with robust weighting. The noise per 2.601 km s^{-1} wide channel is 40 mJy beam^{-1} in the combined data of both tracks. For the intensity map, we used only emission that is 5 σ above the noise floor and evident in at least two adjacent channels. Similarly, we used a 15 σ blanking for the velocity field to emphasize the small-scale velocity structure. Nevertheless, our data recover most of the CO flux in the region mapped, as the peak integrated intensity of our data convolved to 14″ resolution is about 90% of the value of $I_{30\,m} = 324$ K km s^{-1} measured with the IRAM 30 m single-dish telescope (Eckart et al. 1990). The absolute astrometry of the OVRO observations are tied to the Very Large Array quasar reference frame, which is known to ≤0″.02. However, the positional uncertainty in the observations is limited by atmospheric refraction at 230 GHz and is less than 0″.1.

For comparison to the CO data, we retrieved *HST* V-band (F555W) and Hα (+continuum, F658N) maps from the newly available Wide Field Planetary Camera 2 associations archive. In order to register the *HST* images and the CO maps, we

---

[1] National Radio Astronomy Observatory, P.O. Box O, Socorro, NM 87801.
[2] Jansky Fellow.
[3] Space Telescope Science Institute, 3700 San Martin Drive, Baltimore, MD 21218.
[4] On assignment from the Space Telescope Division of the European Space Agency (ESA).
[5] University of Illinois at Urbana-Champaign, 1002 West Green Street, Urbana, IL 61801.
[6] The distance to IC 342 is uncertain; e.g., more recent observations indicate a larger distance of 3.3 Mpc (Saha, Claver, & Hoessel 2002). This should be kept in mind when discussing distance-dependent quantities.
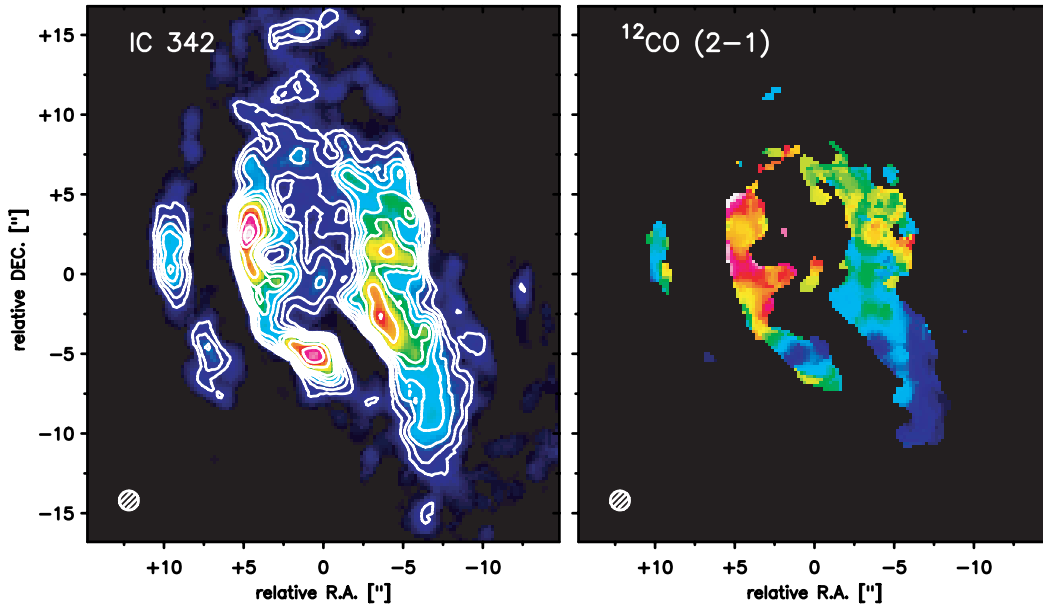
Fig. 1.—OVRO ^{12}CO (2–1) intensity map (*left*) and velocity field (*right*) at 10 pc (1″2) resolution. The contours in the intensity map are at 4, 6, 8, 10, 12, 14, 18, 22, and 26 σ (1 σ = 2.6 Jy beam^{-1} km s^{-1}). The coordinate center is at R.A. = $03^h46^m48^s26$, decl. = $+68°05'47''8$ (J2000.0). The beam size is shown in the bottom left corner.

aligned the eastern CO spiral arm to the prominent dust lane seen in both *HST* images. Incidentally, this also aligned the central CO peak with the nuclear star cluster. The alignment required a nominal shift of 1″28 to the west and 0″59 to the north.[7] Potential discrepancies of this magnitude between *HST* and radio coordinate systems are not uncommon (e.g., Whitmore & Zhang 2002).

3. MOLECULAR GAS PROPERTIES

CO *distribution and geometry*.—The intensity map in Figure 1 partly resolves the structure of the two well-known molecular spiral arms (e.g., Lo et al. 1984; Turner & Hurt 1992; Meier et al. 2000; Meier & Turner 2001). The two arms have quite different morphologies: the eastern arm forms a continuous spiral that is barely resolved with our data. A second, weaker component about 5″ east of the main arm is also apparent in the map. The western arm, on the other hand, has two main components: a southern part pointing toward the nucleus and a northern part (north of $-3''$, $0''$) that seems to form another spiral. The western arm is about 5″ wide and has a sharp inner edge but becomes more diffuse toward larger radii. The mean gas density within the spiral arms is $\sim10^{23}$ cm^{-2}, assuming an intrinsic line ratio of $I_{21}/I_{10} = 1$ and the standard Galactic conversion factor of 2×10^{20} cm^{-2} (K km s^{-1})$^{-1}$ (Strong et al. 1988). These values translate into average gas surface densities of ~1100 $M_\odot$ pc^{-2} (including a 36% contribution from He), with peak values about twice as high. The map reveals somewhat weaker emission inside the central trough that has been identified for the first time. Because this emission component has a disklike morphology and appears centered on the nuclear star cluster (see below), we refer to it as the nuclear disk for the remainder of this Letter. The disk has a major-axis diameter of ~30 pc and a gas mass of $\sim1.7 \times 10^5$ $M_\odot$, with a mean gas density about half of that in the spiral arms. The disk appears connected to both

---

[7] The *HST* coordinates were measured from the positions of eight stars in the field of view that are listed in the USNO-A2.0 catalog.

spiral arms via two faint CO "bridges" $\sim1''$ north and south of the nucleus.

CO *kinematics*.—The overall motion of the molecular gas is from southwest to northeast, in agreement with the position angle of the kinematic major axis of $\sim37°$ determined from H I data (Crosthwaite et al. 2001). The arms of the gas spiral show strong streaming motions and are interpreted as gas lanes along the leading side of a weak stellar bar (Turner & Hurt 1992; Sakamoto et al. 1999). On smaller scales, the CO velocity field within the spiral arms (Fig. 1) does not appear well ordered, since the line emission consists of multiple components. The high spatial and spectral resolution of the OVRO data allows us to identify noncircular gas motions close to the center of IC 342. The molecular gas is moving along a position angle of $\sim-10°$ (Figs. 1 and 2), which is offset by $\sim45°$ from the kinematic major axis of the galaxy disk. This is the first time that noncircular motions within 10 pc of the nucleus have been detected in IC 342; their nature is discussed further in § 4.

Within the spatial resolution of our observations, the central CO peak coincides with the dynamical center as well as the nuclear star cluster, and the systemic velocity that we measure is $v_{\rm LSR} \approx 46.0$ km s^{-1}. This value is ~7 km s^{-1} higher than inferred from lower resolution CO (1–1) data (~39 km s^{-1}; Sakamoto et al. 1999). This discrepancy is likely due to the noncircular nature of the nuclear CO kinematics, which becomes more apparent only at high angular resolution.

Comparison to optical morphology.—The distribution of the molecular gas differs from that of the stellar inventory, as demonstrated by the comparison of the *HST* images to the CO distribution (Fig. 3). The CO spiral arms outline the bright central emission region that is evident in both the Hα emission and the *V*-band continuum. Both the line emission and the optical continuum are brighter east of the nucleus where the CO emission is confined to the prominent dust lane. In addition, optical light fills the gap between the two eastern gas lanes. On the other hand, west of the nucleus where the CO spiral is much wider, there is a lack of Hα emission and optical con-
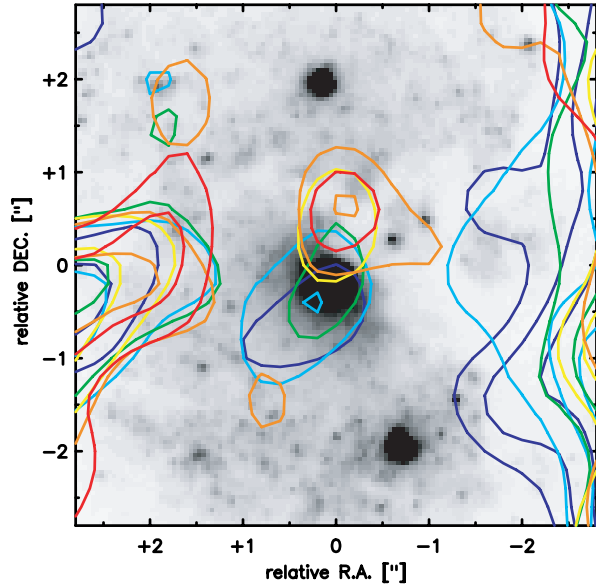
FIG. 2.—Renzogram of ^{12}CO (2–1) emission. Close to the nucleus, the gas is moving along a position angle of $\sim -10°$. The contours represent different channel maps from 41.523 km s^{-1} (*blue*) to 54.528 km s^{-1} (*red*) in steps of 2.601 km s^{-1}. The contours for each channel map are at 15, 20, and 25 σ with $\sigma = 40$ mJy beam^{-1}. The *HST* F555W image is shown in gray scale.

tinuum. This asymmetry in the extinction pattern together with the velocity field suggests that the western side is the near side of IC 342. A prominent Hα knot lies on the boundary ($-3''$; $-1''$) between the two parts of the western gas spiral; it coincides with region 1 studied by Böker et al. (1997) and is the site of intense star formation. Within the nuclear disk, the peak of the molecular gas (which is close to the dynamical center) coincides roughly with the nuclear star cluster. Two other star clusters north and south of the nucleus fall into regions inside the spiral arms that are almost devoid of molecular line emission. The *HST* V-band image shows two fine dust lanes of $\sim 0''.2$ width about $1''$ north and south of the nucleus that extend in the east-west direction (best seen in Fig. 2). The two CO bridges that connect the nuclear disk to the spiral arms appear to coincide with these dust lanes, although the lower spatial reso-

lution of the CO map makes this identification somewhat tentative.

4. DISCUSSION

What drives the gas inflow?—The overall shape and kinematics of the CO spiral arms are reminiscent of models for gas flows in a weakly barred potential (e.g., Athanassoula 1992). Although no stellar bar is obvious in the optical data, ellipse fits to deep wide-field CCD images show evidence for a bar with a length of $600''$–$700''$ and a position angle of $\sim 20°$ (Buta & McCall 1999). Since the western side is the near side (see § 3), the sense of rotation is counterclockwise, and therefore the gas spiral arms are on the leading side of this large-scale bar. Crosthwaite et al. (2001) interpret the displacement of the optical and dynamical position angles and the warped outer H I disk as signs of a recent mild interaction. This interaction might have triggered the formation of the oval distortion, which in turn might be responsible for the pileup of molecular gas in the central kiloparsec of IC 342. The molecular gas morphology of IC 342 is quite similar to the one observed in the center of our own Galaxy, where a ~ 14 pc wide molecular disk or torus is surrounded by a molecular ring with a radius of 180 pc (see review by Morris & Serabyn 1996). Also, the bar length of ~ 5.2 kpc in IC 342 is comparable to the 4.8 kpc observed in our Galaxy. The filamentary structure of the dust/gas lanes and the Hα emission in IC 342 (similar filaments are also observed in the inner 500 pc of our Galaxy) might be explained by self-gravitating gas (see Fig. 2 of Wada & Koda 2001). The coincidence of the CO disk's central velocity with systemic velocity favors a scenario in which the gas lies within the disk, as opposed to being situated above the plane. The in-plane picture is supported by the good agreement between the gas distribution and the dust morphology.

In the following, we discuss three plausible interpretations of the CO morphology. First, the nuclear CO disk could be tilted relative to the large stellar disk. The axis ratio of the nuclear disk of $b/a \sim 0.5$ translates into an inclination of $i \sim 60°$ along a position angle of $\sim 15°$. The two CO peaks about $0''.5$ north and south of the center are separated in velocity by 8 km s^{-1} (see Fig. 2). Assuming solid-body rotation and that these two peaks fall on the kinematic major axis of the nuclear disk, the resulting dynamical mass is $M_{\rm dyn} \sim 2 \times 10^4 \, M_\odot$. The
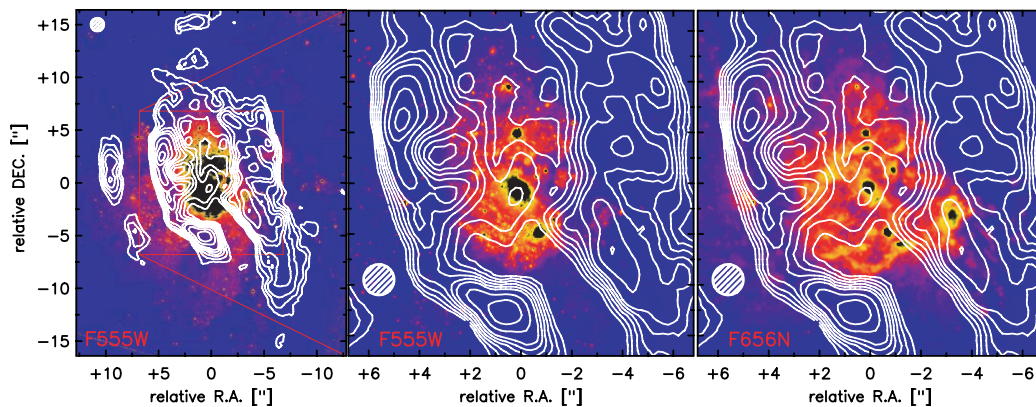

FIG. 3.—The OVRO ^{12}CO (2–1) intensity map overlaid onto the archival *HST* V-band (*left and middle*) and Hα (*right*) images. The left panel shows the full OVRO field, while the middle and right panels contain only the inner 120 pc (indicated by a red box in the left panel). Different color stretches are used to enhance low-level emission (*left*) as well as distinct features in the nuclear region (*middle*) of the *HST* F555W image. The OVRO CO contours are the same as in Fig. 1. For reference, the beam size is shown in each panel.

derived mass is significantly smaller than the mass estimated for either the nuclear molecular gas disk or the nuclear stellar cluster ($6 \times 10^6 \, M_\odot$; Böker et al. 1999), making this an unlikely scenario. A second alternative is that the nuclear CO emission originates in a virialized cloud, rather than a rotating disk. For a cloud size of about $2''$ (17 pc) and a CO line width (FWHM) of $\Delta v \sim 8$ km s^{-1}, the virialized mass is $M_{\rm vir} \sim 3 \times 10^5 \, M_\odot$. However, the observed rotation (see Fig. 2) within the nuclear disk argues against a single virialized cloud. In a third scenario, the observed noncircular motions are due to radial motions of material moving toward the center, similar to what is observed in the central region of our Galaxy (Morris & Serabyn 1996). Since the first two scenarios seem unlikely, we conclude that streaming motions are the most plausible explanation for the noncircular motions observed in the CO kinematics. A possible cause for such streaming motion could be the large-scale stellar bar. This scenario should be investigated further by dynamical modeling.

Feeding the nuclear star cluster.—The nuclear star cluster in IC 342 has a mass of $6 \times 10^6 \, M_\odot$ and experienced a major burst of star formation ~ 60 Myr ago (Böker et al. 1999). The population of stars produced in this event dominates the SED of the cluster and thus makes it difficult to quantify the contribution from possible older generation(s) of stars. As discussed in Böker et al. (1999), up to 90% of the cluster mass could have been produced in a burst that occurred 10 Gyr before the most recent one. While this number is definitely an upper limit because the described scenario lies at the extreme end of possible star formation histories, it is reasonable to assume that previous nuclear starburst events have indeed occurred. For the moment, we will assume that the most recent burst produced 30% of the cluster mass, i.e., about $2 \times 10^6 \, M_\odot$. Assuming a star formation efficiency of 20% (Elmegreen et al. 1999), about $10^7 \, M_\odot$ of molecular gas is needed in order to produce such a starburst event. This is 50 times more than the present-day mass of the nuclear CO disk ($M_{\rm H_2} \sim 1.7 \times 10^5 \, M_\odot$). In what follows, we use our CO observations to constrain the inflow rate of molecular gas and to estimate how long it might take before another such starburst event can occur.

A lower limit can be calculated by assuming that it took the full 60 Myr since the last starburst for the nuclear CO disk to form. In this case, the inflow rate is $\sim 0.003 \, M_\odot$ yr^{-1}, so about 3 Gyr are needed before a new starburst event could occur. We derive an upper limit by taking the observed gas surface density of $\Sigma \sim 500 \, M_\odot$ pc^{-2} together with the width of the two dust lanes seen in the V-band image ($\sim 0''.2$). This yields an estimate of the gas inflow rate onto the nuclear disk of $\sim 2000 \, M_\odot$ pc$^{-1} \times v_{\rm rad}$. The inflow velocity of the gas, $v_{\rm rad}$, can be estimated

by comparing the observed circular velocity in the nuclear disk ($v_{\rm obs} \approx 25$ km s^{-1} at a radius of $0''.5$ or 4.4 pc) to the maximum expected circular velocity around the nuclear star cluster (assuming solid-body rotation), $v_{\rm sb} \approx 75$ km s^{-1}. This implies that radial motions of up to $v_{\rm rad} \sim 70$ km s^{-1} can be present in the molecular gas next to the nuclear cluster, depending on the exact shape of the gravitational potential. These rough estimates result in an inflow rate of $\sim 0.14 \, M_\odot$ yr^{-1}. Such an inflow rate would accumulate about $10^7 \, M_\odot$ of molecular gas in the nucleus within 70 Myr.

These two estimates probably bracket the actual inflow rate, but a number of uncertainties remain. For one, the H$_2$ mass in the center of IC 342 might be overestimated by a factor of 4–5 because of the use of a Galactic conversion factor, as discussed in Meier & Turner (2001). In addition, the noncircular motions can be overestimated because of the unknown shape of the underlying gravitational potential. Nevertheless, the inflow rates discussed here are not unreasonable to support repetitive nuclear starbursts in IC 342.

For example, an accumulation rate of $\sim 0.01 \, M_\odot$ yr^{-1} is sufficient to support a starburst duty cycle of about 1 Gyr. The duty cycle might even be shorter if the star formation efficiency is higher than the 20% assumed here. Indeed, efficiencies up to 50% have been inferred for giant molecular clouds in the spiral arms of IC 342 (Meier & Turner 2001). Moreover, the inflow rate is likely to vary over time with lower inflow rates in the past and could increase in the future as more mass is accumulated at the center. For example, assuming a constant rate of $0.003 \, M_\odot$ yr^{-1} (our lower limit) over a Hubble time (10^{10} yr) results in a mass accumulation of $\sim 3 \times 10^7 \, M_\odot$, which is larger than the dynamical mass of $\sim 2 \times 10^7 \, M_\odot$ derived for the central 120 pc (Turner & Hurt 1992).

Our analysis of new high-resolution maps of the ^{12}CO (2–1) emission in the center of IC 342 has revealed the following main results. We detect molecular gas coinciding with the nuclear stellar cluster. This, and the presence of streaming motions close to the nucleus, suggests that gaseous matter is currently accumulating at the nucleus of IC 342. These findings provide support for in situ formation of nuclear clusters and repetitive nuclear starbursts. Rough estimates of gas inflow rates suggest that massive ($10^6 \, M_\odot$) nuclear starbursts in IC 342 can be supported with duty cycles between a few hundred megayears and 1 Gyr.

REFERENCES

Athanassoula, E. 1992, MNRAS, 259, 345
Böker, T., Förster-Schreiber, N. M., & Genzel, R. 1997, AJ, 114, 1883
Böker, T., Laine, S., van der Marel, R. P., Sarzi, M., Rix, H.-W., Ho, L., & Shields, J. C. 2002, AJ, 123, 1389
Böker, T., van der Marel, R. P., Mazzuca, L., Rix, H.-W., Rudnick, G., Ho, L., & Shields, J. C. 2001, AJ, 121, 1473
Böker, T., van der Marel, R. P., & Vacca, W. D. 1999, AJ, 118, 831
Buta, R. J., & McCall, M. L. 1999, ApJS, 124, 33
Carollo, C. M., Stiavelli, M., & Mack, J. 1998, AJ, 116, 68
Crosthwaite, L. P., Turner, J. L., Hurt, R. L., Levine, D. A., Martin, R. N., & Ho, P. T. P. 2001, AJ, 122, 797
Davidge, T. J., & Courteau, S. 2002, AJ, 123, 1438
Eckart, A., Downes, D., Genzel, R., Harris, A. I., Jaffe, D. T., & Wild, W. 1990, ApJ, 348, 434
Elmegreen, B. G., Efremov, Y., Pudritz, R. E., & Zinnecker, H. 1999, in Protostars and Planets IV, ed. V. Mannings, A. P. Boss, & S. S. Russell (Tucson: Univ. Arizona Press), 179

Gordon, K. D., Hanson, M. M., Clayton, G. C., Rieke, G. H., & Misselt, K. A. 1999, ApJ, 519, 165
Ishizuki, S., Kawabe, R., Ishiguro, M., Okumura, S. K., & Morita, K. 1990, Nature, 344, 224
Lo, K. Y., et al. 1984, ApJ, 282, L59
McCall, M. L. 1989, AJ, 97, 1341
Meier, D. S., & Turner, J. L. 2001, ApJ, 551, 687
Meier, D. S., Turner, J. L., & Hurt, R. L. 2000, ApJ, 531, 200
Morris, M., & Serabyn, E. 1996, ARA&A, 34, 645
Saha, A., Claver, J., & Hoessel, J. G. 2002, AJ, 124, 839
Sakamoto, K., Okumura, S. K., Ishizuki, S., & Scoville, N. Z. 1999, ApJS, 124, 403
Strong, A. W., et al. 1988, A&A, 207, 1
Turner, J. L., & Hurt, R. L. 1992, ApJ, 384, 72
Turner, J. L., Hurt, R. L., & Hudson, D. Y. 1993, ApJ, 413, L19
Wada, K., & Koda, J. 2001, PASJ, 53, 1163
Whitmore, B. C., & Zhang, Q. 2002, AJ, 124, 1418